ARCHITECTURAL RESEARCH, Vol. 7, NO. 1 (2005), pp. 39-48

Effects of Transverse Reinforcement on Strength and Ductility of High-Strength Concrete Columns

Sun Kyoung Hwang, Byung Hoon Lim, Chang Gyo Kim
Department of Architecture,Woosong University, Daejeon, Korea
Hyun Do Yun and Wan Shin Park
Department of Architectural Engineering, Chungnam National University, Daejeon, Korea

Abstract

Main objective of this research is to evaluate performance of high-strength concrete (HSC) columns for ductility and strength. Eight one-third scale columns with compressive strength of 69 MPa were subjected to a constant axial load corresponding to 30 % of the column axial load capacity and a cyclic horizontal load-inducing reversed bending moment. The variables studied in this research are the volumetric ratio of transverse reinforcement (ρ_s=1.58, 2.25 %), tie configuration (Type H, Type C and Type D) and tie yield strength (f_{yh} =549 and 779 MPa). Test results show that the flexural strength of every column exceeds the calculated flexural capacity based on the equivalent concrete stress block used in the current design code. Columns with 42 % higher amounts of transverse reinforcement than that required by seismic provisions of ACI 318-02 showed ductile behaviour, showing a displacement ductility factor ($\mu_{\Delta u}$) of 3.69 to 4.85, and a curvature ductility factor ($\mu_{\varphi u}$) of over 10.0. With an axial load of 30 % of the axial load capacity, it is recommended that the yield strength of transverse reinforcement be held equal to or below 549 MPa.

Keywords: high-strength concrete, tied columns, transverse reinforcement, ductility, strength

1. INTRODUCTION

The literature has documented application of high-strength concrete (HSC) building columns [1]. Many studies [2] have demonstrated the economy of using HSC in columns of high-rise buildings; however, the use of HSC has not been limited to high-rise buildings. Studies [3] indicate that HSC also enhances the economy of low- to mid-rise buildings. In addition to reducing column size and producing a more durable material, use of HSC has been shown to be advantageous with regard to lateral stiffness and axial shortening.

In recent years, there has been some corcern regarding the use of HSC in building columns in seismic areas. The application of HSC in high seismic regions has lagged behind its application in regions of low seismicity. One of the primary reasons has been concern over the ductility of HSC columns subjected to seismic forces.

Seismic-resistant design of reinforced ductile frame buildings [4], provides the mandate condition of a strong column and weak beam at any junction. The intent is to encourage hinging in the beams rather than in the columns. However, building performance during seismic activity indicates that hinging can occur in columns. Therefore, the possibility of plastic hinge formation at column ends demands that building columns in seismic areas have sufficient ductility.

Sakai and Sheikh[5] have summarized major research conducted on the subject of confinement of concrete columns constructed using NSC. However, information on the ductility of HSC columns has been limited[6-7], with most of the available information being based on experimental testing of small-scale columns subjected to concentric axial loads only. ACI-ASCE Committee 441[8] pointed out that columns subjected to axial loads of less than 20 % of column axial-load capacity exhibited a good level of ductility when confined according to current ACI confinement requirements. The scientific community has not yet reached a consensus on required confinement reinforcement for ductile HSC columns.

This experimental investigation was conducted to examine the seismic behaviour of eight one-third scale HSC columns. The columns were subjected to a constant axial load corresponding to 30 % of the column axial-load capacity and a cyclic horizontal load-inducing reversed bending moment. The variables studied in this research were the volumetric ratio of transverse reinforcement, tie configuration and tie yield strength.

2. SPECIMENS

The dimensions and steel-bar-reinforcement layout of the reinforced concrete column are shown in Fig. 1. Each specimen consisted of a 200×200×600 mm column cast integrally with a 400×500×400 mm stub. The core size measured from the centre of the perimeter tie was kept constant at 174×174 mm for all specimens, giving a core area equal to 72 % of the gross area of the column. Table 1 includes details of the test specimens. Each specimen contained eight D13 longitudinal bars providing a reinforcement ratio of 2.54 % of the gross-sectional area of the column. Yield strength of the longitudinal steel was 431 MPa. The volumetric ratio of transverse reinforcement to concrete core, measured centre-to-centre of perimeter ties, varied between 1.58 % and 2.25 %, and spacing of the ties varied between 27 mm and 65 mm. Type C transverse reinforcement consisted of φ6 peripheral hoops and cross ties. Type D transverse reinforcement consisted of φ6 peripheral hoops and diagonal hoops. However, Type H transverse reinforcement consisted only of ϕ 6 peripheral hoops (Fig. 2).

S-series consisted of three specimens that were designed

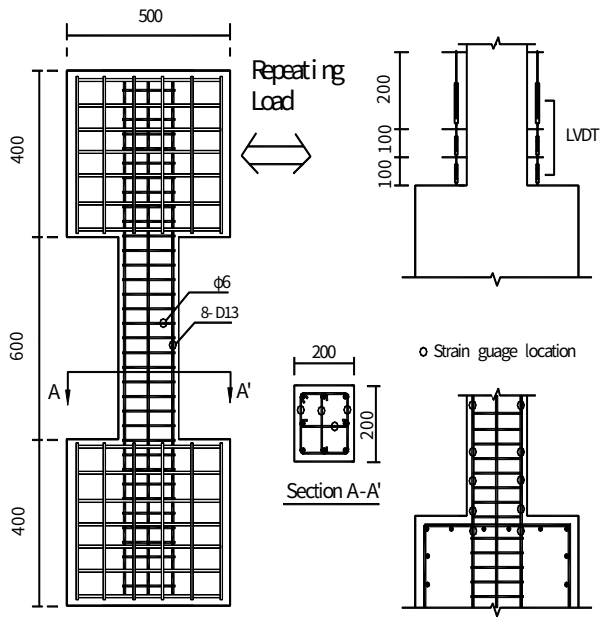

Figure 1. Detail of Specimens and gaging arrangements (Unit : mm)

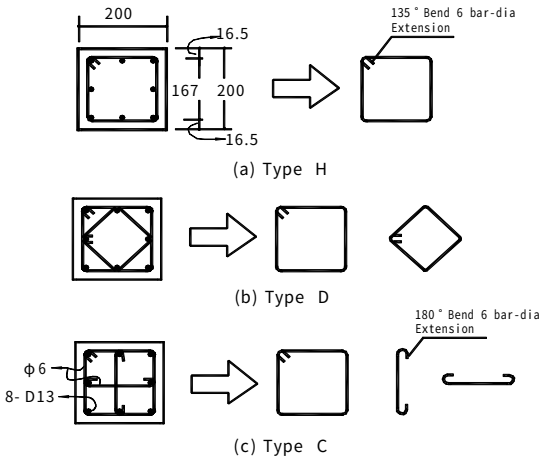

Figure 2. Tie shape (Unit : mm)

in accordance with the provision ACI 318-02 and reinforced with a high yield strength (779 MPa) of transverse steel. For S-series, the spacing of lateral steel was 38 for Type H, 57 for Type C, and 65 mm for Type D (Fig. 2).

(1) Materials

Ready-mix normal-weight concrete with an average slump of 210 mm was used. Forty-eight standard cylinders were cast with the specimens, and tested at 3, 7, 14, 21, 28, and 42 days, and also during testing to monitor the strength of concrete. The 7-day strength of concrete was about 75 % of the 28-day concrete strength (Table 2), and afterwards, the 28-day concrete strength increased by about 10 % in the following six months. The measured compressive strengths of concrete cylinders at the date of testing are listed in Table 1. Two different types of reinforcing steel were used to construct specimens. Important properties of steel are also listed in Table 3. The parameters f_y and f_u represent the yield strength and ultimate strength, respectively; ε_y represent strain values at the onset of yield.

(2) Instrumentation and test procedures

Several electrical strain gauges were placed in the specimens on both the longitudinal and transverse bars (Fig. 1). Three or four sets of ties just above the stub were instrumented with electrical strain gauges. Curvatures were calculated from the readings of three sets of six linear variable displacement transducers (LVDTs). The LVDTs were supported by steel rods passing through the core and extending from one side of the column to the other.

Test setup and loading conditions are shown schematically in Fig. 3. Axial compression in the column was applied by a 980 kN hydraulic jack. The horizontal load was applied with a 490 kN hydraulic jack. The applied horizontal force was measured by a load cell. The horizontal tip displacement was measured by an LVDT with a range of 300 mm. The test began with application of the axial load at the targeted value. For the first cycle of loading, the horizontal force reached 75 % of the expected yield load.

Table 1. Properties of specimens

Specimen	Transverse reinforcement						Longitudinal bar			f_{ck} (MPa)	Set
	Bar	S (mm)	Detail (1)	ρ_s (2) (%)	$\frac{\rho_S}{\rho_{(ACI)}}$	f_{yh} (MPa)	Bar	f_y (MPa)	ρ_t (%)		
C-S	Φ6	57	C	1.58	1.00	779.10	8-D13	430.71	2.54	68.60	S-series
D-S	Φ6	65	D	1.58	1.00	779.10	8-D13	430.71	2.54	68.60	
H-S	Φ6	38	H	1.58	1.00	779.10	8-D13	430.71	2.54	68.60	
C-A	Φ6	40	C	2.25	1.42	779.10	8-D13	430.71	2.54	68.60	A-series
D-A	Φ6	46	D	2.25	1.42	779.10	8-D13	430.71	2.54	68.60	
H-A	Φ6	27	H	2.25	1.42	779.10	8-D13	430.71	2.54	68.60	
L-C-S	Φ6	40	C	2.25	1.00	548.80	8-D13	430.71	2.54	68.60	L-series
L-D-S	Φ6	46	D	2.25	1.00	548.80	8-D13	430.71	2.54	68.60	

(1) Details of transverse reinforcements (C: Type C, D: Type D, H: Type H)

(2) Ratio of transverse reinforcement over spacing S to core volume of concrete confined by transverse reinforcement (measure out-to-out)

Table 2. Concrete compressive strengths

Average strength (MPa)					E_c (MPa)
Age (days)	7	10	21	28	33,124
Strength (MPa)	51.16	58.60	63.41	68.70	

Table 3. Properties of reinforcement

	E_s (MPa)	f_y (MPa)	ε_y ($\times 10^{-6}$)	f_u (MPa)	Elongation (%)
D13	175626	430.71	2,448	564.87	18.00
Φ6	202860	779.10	5,700	847.70	15.20
Φ6	205800	548.80	4,600	586.04	13.80

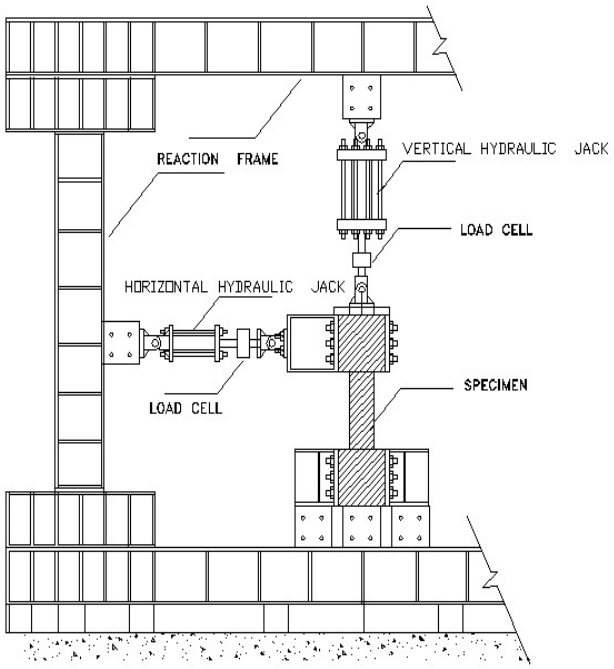

Figure 3. Test setup and loading condition

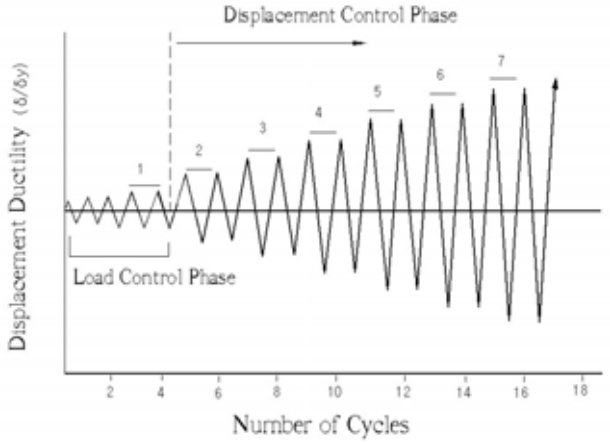

Figure 4. Lateral displacement sequence

The second cycle reached the yield load, and the yield displacement was defined as the point at which longitudinal bars first yield. Thereafter, each cycle was under displacement control with a maximum displacement equal to 2,3,4…, times the measured yield displacement up to failure (Fig. 4). All the experimental data were stored at predetermined steps and recorded at special occurrences such as cracking, and yielding.

3. TEST RESULTS

(1) Test observations

In all the specimens, the first crack occurred in the direction perpendicular to the column axis in the plastic hinge region at lateral force of 0.5 V_{if}. As lateral force increased, flexural cracking spread to 50 % of the distance from the critical sections between the bottom end and the lateral loading point. Afterward, the inclined cracks were noted at lateral force of 0.85 V_{if}. At a displacement ductility of $\mu_\Delta = 1$, the longitudinal bars yielded in tension. Incipient spalling of concrete developed in the plastic hinge region at a displacement ductility of $\mu_\Delta = 3$. Spalling of cover extended as displacement increased (Fig. 5).

In most cases, during the last cycle, buckling of the longitudinal bars was observed after yielding of the perimeter ties (Fig. 6), which was an indication of the commencement of failure. The failure of the specimen was accompanied by extensive buckling of the longitudinal bars in all specimens. The failure mode for all specimens was dominated by flexural effects.

(2) Hysteretic loops

Lateral force-displacement hysteresis loops for the eight columns are shown in Fig. 7; this includes lateral force V_{if} at ideal flexural strength based on ACI 318-02 provisions, assuming rectangular concrete stress blocks, and shear force V_y at final yield of longitudinal reinforcement.

The response for the A-series [Fig. 7(a),(c),(e)], with 42 % higher amounts of transverse reinforcement than those required by seismic provisions of ACI 318-02, indicates a more ductile response than for the S-series up to $\mu_\Delta = 4$ or 5. This is a result of the high transverse reinforcement, which enabled transverse steel to effectively confine the core concrete, thus reducing the drastic degradation of lateral strength. The maximum lateral force was between 84 and 92 kN, and the index V_{max} / V_{if}, varied from 0.93 to 1.02.

The response for the S-series [Fig. 7(b),(d),(f)], with the amounts of transverse reinforcement required by seismic provisions of ACI 318-02, indicates a ductile response up to $\mu_\Delta = 3$ or 4. On further loading to displace the specimens beyond $\mu_\Delta = 4$, sudden degradation in strength and stiffness occurred. Excessive widening of diagonal cracks caused loss of aggregate interlock capacity and hence, demanded more contribution from transverse reinforcement to carry the applied lateral force. The maximum lateral force was between 92 and 98 kN, and the index V_{max} / V_{if}, varied

(a) after 2 cycle to μ = 2 (R=0.0083 rad)

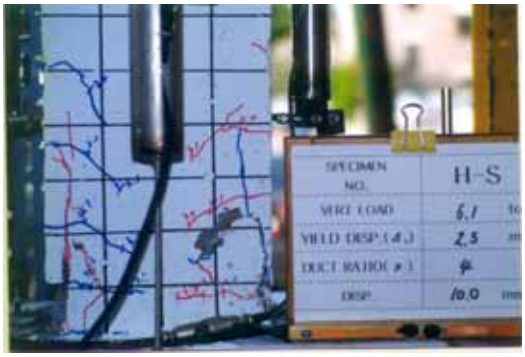

(b) after 2 cycle to μ = 4 (R=0.0166 rad)

(c) at the end of testing

Figure 5. Column H-S at each stage of testing

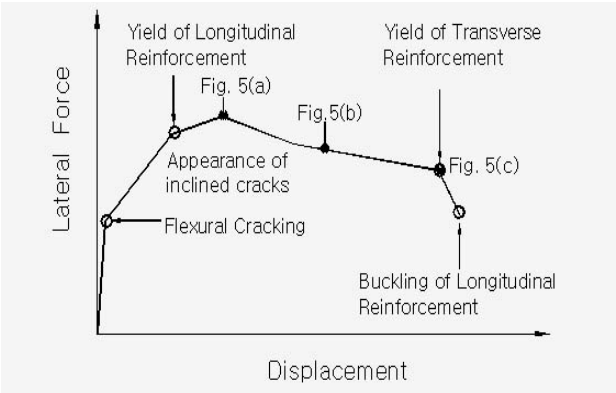

Figure 6. Summary of observed behaviour

from 1.02 to 1.08, which exceeded the ideal lateral force as a consequence of strain hardening of longitudinal reinforcement.

The response for the L-series [Fig. 7(g),(h)], with a low yield strength (549 MPa) of transverse reinforcement, which satisfies seismic provisions of ACI 318-02, indicates a ductile response up to $\mu_\Delta = 4$. The maximum lateral force was between 87 and 91 kN, and the index V_{max} / V_{if}, varied from 0.96 to 1.01.

(3) Ductility factor and energy dissipation

To quantify the response of columns, it is desirable to define response indices that quantitatively describe the columns' behaviour. In seismic design, the inelastic deformation is generally quantified by ductility parameters and by energy dissipation capacity. For long-period structures, it has been stated that ductility is directly related to the strength reduction factor used in most codes [9] to calculate the seismic base shear. The energy dissipation capacity is an important parameter in the design of short-period structures and structures subjected to a long-duration earthquake. The energy dissipation capacity also accounts for the history of loadings in addition to the maximum displacement attained. Both types of indicators are computed in this paper to compare the column behaviour on a rational basis.

Because the behaviour of reinforced concrete structures is not elastic-perfectly plastic, it has been the general practice to define ductility parameters from a conventional diagram [10,11]. Hence, the load-displacement behaviour is idealized as a bilinear diagram, consisting of an elastic branch and an inclined post-elastic branch [Fig. 8(a)]. The elastic branch is secant to the real curve at 75 % of maximum horizontal load, and reaches the maximum horizontal load to define the yield displacement for Δ_{yI}. The failure of the column is conventionally defined at the post-peak displacement Δ_2, where the remaining capacity of the column has dropped to 80 % of the peak load. The idealized post-elastic branch starts at point (Δ_{yI}, H_{max}) and goes to (Δ_2, H_2). H_2 is defined so that the idealized diagram and the real envelope curve have the same area under the curve, thus ensuring equal energy criteria. The sectional behaviour in terms of a moment–curvature diagram is idealized using the same procedure [Fig. 8(b)]. The ductility parameters are defined from the idealized diagrams.

The ultimate displacement ductility is defined as

$$\mu_{\Delta u} = \frac{\Delta_2}{\Delta_{yI}} \tag{1}$$

and the ultimate curvature ductility is defined as

$$\mu_{\Phi u} = \frac{\Phi_2}{\Phi_{yI}} \tag{2}$$

A column is generally considered ductile if displacement ductility ranges from 4 to 6. Table 4 provides the values of $\mu_{\Delta u}$ and $\mu_{\varphi u}$ for each column.

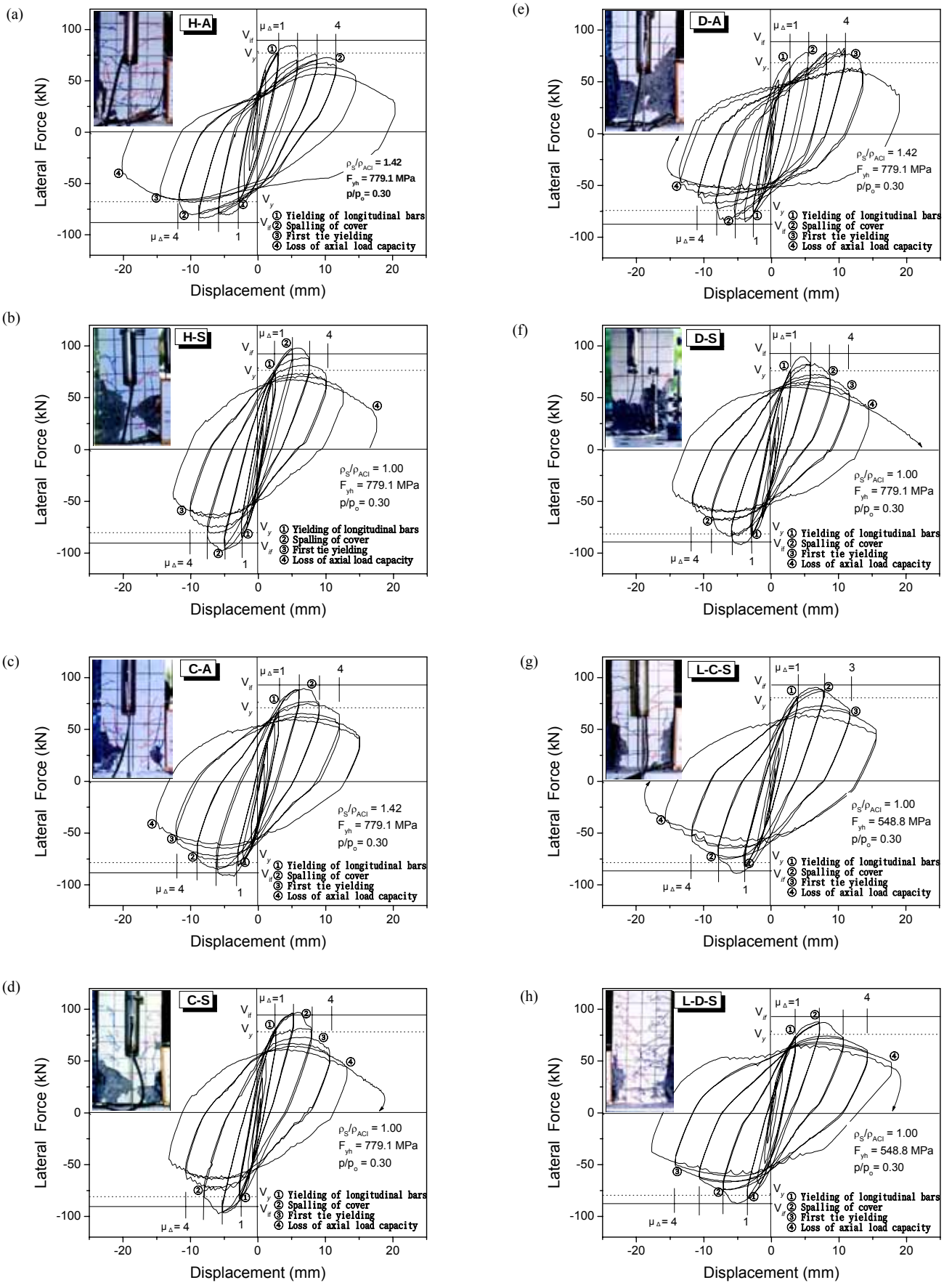

Figure 7. Lateral load-displacement response

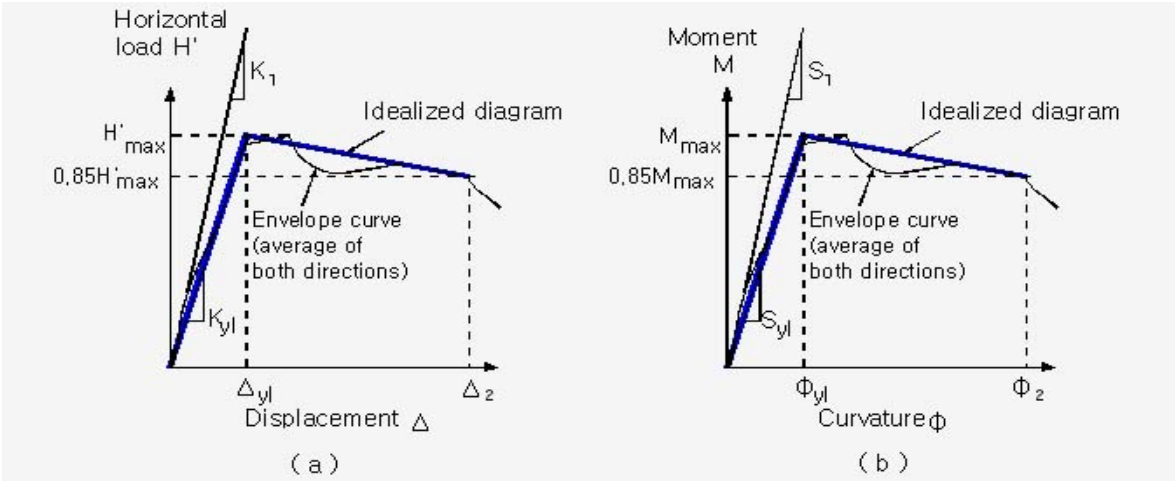

Figure 8. Idealized curvature definitions

Table 4. Summary of test results

Specimen	S (mm)	Detail	ρ_s (%)	$\frac{\rho_S}{\rho_{(ACI)}}$	f_{yh} (MPa)	Δ_{yl} (mm)	Φ_{yI} ($\times 10^{-4}$ rad/mm)	Δ_2 (mm)	Φ_2 ($\times 10^{-4}$ rad/mm)	$\mu_{\Delta u} = \frac{\Delta_2}{\Delta_{yI}}$	$\mu_{\varphi u} = \frac{\Phi_2}{\Phi_{yI}}$	E_N
C-S	57	C	1.58	1.00	779	2.35	0.17	7.64	1.66	3.25	9.75	7.8
D-S	65	D	1.58	1.00	779	1.76	0.16	5.56	1.44	3.16	9.00	7.7
H-S	38	H	1.58	1.00	779	2.35	0.17	8.34	2.45	3.55	14.40	7.9
C-A	40	C	2.25	1.42	779	2.31	0.15	8.52	2.25	3.69	15.00	9.5
D-A	46	D	2.25	1.42	779	3.11	0.20	13.62	3.56	4.38	17.80	9.6
H-A	27	H	2.25	1.42	779	2.61	0.15	12.66	2.97	4.85	19.80	9.7
L-C-S	40	C	2.25	1.00	549	2.26	0.20	8.23	2.94	3.64	14.70	10.0
L-D-S	46	D	2.25	1.00	549	2.36	0.21	8.73	3.15	3.70	15.0	11.4

The energy dissipation is defined for a cycle *i* by the hatched area in Fig. 9, or mathematically by

$$E_i = \int_A^B H' d\Delta \tag{3}$$

The total energy dissipated during the test until 80 % conventional failure is

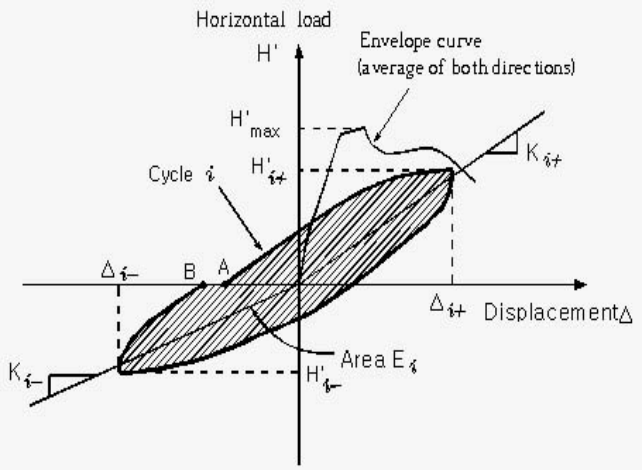

Figure 9. Energy dissipation

$$E_{hyst} = \sum_{i=1}^{n} E_i \tag{4}$$

where n is the number of cycles to failure. For comparison purposes, it is convenient to normalize the dissipated energy

$$E_N = \frac{1}{H'_{\max} \Delta_{yI}} \sum_{i=1}^{n} E_i \tag{5}$$

where E_N is the normalized dissipated energy. To determine E_N, only cycles occurring before conventional failure are taken into account. These data are provided for each specimen in Table 4.

(4) Strain distribution

Figures 10 and 11 show the typical strain distribution for two test columns at different displacement ductility ratios. The yield strain of transverse reinforcement was approximately 2,100 microstrains. As noted in Fig. 10, for specimen C-A, which used higher-yield-strength steel for transverse reinforcement, the yield strain in ties was reached at relatively high displacement (11.55 mm). However, when lower-yield-strength steel for transverse reinforcement was used (Fig. 11), yielding was observed at a horizontal low displacement of 7.91 mm. Therefore, for axial -load

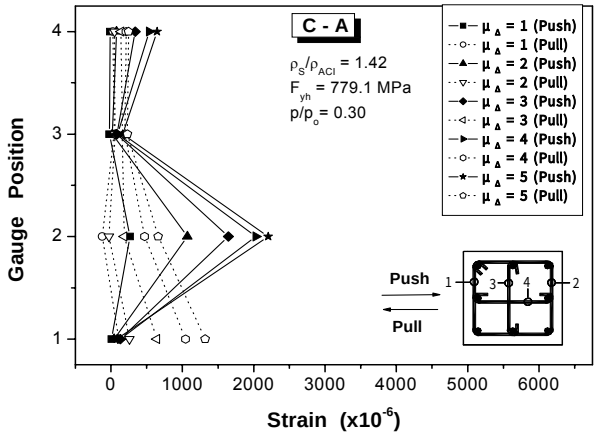

Figure 10. Strain in transverse reinforcement in critical region of test C-A

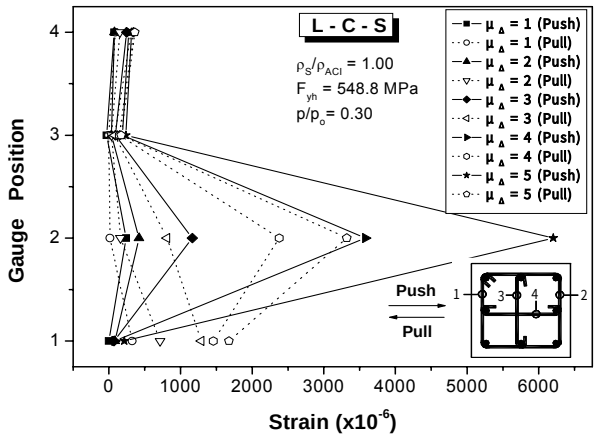

Figure 11. Strain in transverse reinforcement in critical region of test L-C-S

levels below 30% of the column's axial capacity, increasing the yield strength of transverse reinforcement would have little effect.

4. DISCUSSION OF RESULTS

As mentioned previously, the effects of three variables were investigated in the present experimental program: 1) the effect of steel configuration; 2) the volumetric ratio of transverse steel; and 3) the yield strength of transverse steel. It is possible to assess the effect of each variable graphically from Fig. 7. In this figure, HSC columns (f_{ck}=69 MPa) can be made to behave in a ductile manner under intermediate levels of axial load, provided that a sufficient amount of confining steel is used in an efficient configuration. Specimens H-A, C-A, and D-A which had 42 % more steel than the amount listed in the ACI 318-02 requirements, behave in a highly ductile manner, showing a displacement ductility factor ($\mu_{\Delta u}$) of 3.69 to 4.85, and a curvature ductility factor ($\mu_{\varphi u}$) of over 10.0. The noticeable differences between the responses of the tested specimens indicate that confinement is affected greatly by different variables.

1) Effect of steel configuration

The effect of steel configuration on the cyclic behaviour of HSC columns can be examined by comparing the behaviour of specimens C-A, D-A, and H-A, which contained 42 % more steel than ACI 318-02 requirements and were tested under the same level of axial load. Curvature ductility factors ($\mu_{\varphi u}$) of specimen H-A are approximately 11 and 32 % larger than those of specimens C-A and D-A, respectively. Total energy dissipated in specimen H-A, measured by E_N, is a little larger than the energy dissipated in specimens C-A and D-A. Similar conclusions can be drawn from a comparison of the S-series with the amounts of transverse reinforcement required by the seismic provisions of ACI 318-02. Curvature ductility factors ($\mu_{\varphi u}$) of specimen H-S is approximately 48 to 60 % larger than those of specimens C-A and D-A (Table 4).

(2) Effect of the volumetric ratio of transverse steel

The volumetric ratio of confinement steel is assessed on three sets of columns. The first set comprises C-S and C-A. While both specimens are subjected to the same level of axial load, the volumetric ratio of confinement steel is 1.58 % for C-S, and 2.25 % for C-A. Figure 7 illustrates that specimen C-A can sustain larger inelastic cyclic displacement than specimen C-S. The results presented in Table 5 indicate that specimen C-A has a curvature ductility one and a half times that of specimen C-S. The normalized dissipated energy of specimen C-A is 22 % higher than for specimen C-S. The second set comprises D-S and D-A. Both specimens have the same transverse reinforcement as C-S and C-A, respectively. Specimens in the second set, however, used detail D. Figure 7 illustrates that specimen D-A can sustain larger inelastic cyclic displacement than specimen D-S. The curvature ductility of specimen D-A is about twice that of D-S, and the normalized dissipated energy of specimen D-A is 25 % higher than that of specimen D-S. The same observations are made from an examination of the responses (Fig. 7) and the ductility parameters, as well as from the energy dissipation capacity from the third set (specimens H-S and H-A). This experimental program points to the influence of the volumetric ratio of confinement steel as an important parameter in controlling column responses.

(3) Effect of the yield strength of transverse steel

Table 6 shows the results of four test columns that were compared to determine the effect of the yield strength of transverse reinforcement. For these four test columns, the applied axial load was 30 % of each column's axial load capacity. Results indicate that at this axial load level, an increase in the yield strength of the transverse reinforcement had little influence on either the curvature ductility or the normalized dissipated energy E_N.

One reason for using higher strength steel for transverse reinforcement in HSC columns is to allow larger spacing of ties. However, one should be very careful in using this approach, as can be seen by comparing the behaviour of

Table 5. Effect of the volumetric ratio of transverse steel

Group No.	Specimen	S (mm)	Detail	ρ_s (%)	$\frac{\rho_S}{\rho_{(ACI)}}$	Δ_2 (mm)	Φ_2 ($\times 10^{-4}$ rad/mm)	$\mu_{\Delta u} = \frac{\Delta_2}{\Delta_{yI}}$	$\mu_{\varphi u} = \frac{\Phi_2}{\Phi_{yI}}$	E_N
1	C-S	57	C	1.58	1.00	7.64	1.66	3.25	9.75	7.8
	C-A	40	C	2.25	1.42	8.52	2.25	3.69	15.0	9.5
2	D-S	65	D	1.58	1.00	5.56	1.44	3.16	9.0	7.7
	D-A	46	D	2.25	1.42	13.62	3.56	4.38	17.8	9.6
3	H-S	38	H	1.58	1.00	8.34	2.45	3.55	14.4	7.9
	H-A	27	H	2.25	1.42	12.66	2.97	4.85	19.8	9.7

Table 6. Effect of the yield strength of transverse steel

Group No.	Specimen	S (mm)	Detail	$\frac{\rho_S}{\rho_{(ACI)}}$	f_{yh} (MPa)	Δ_2 (mm)	Φ_2 ($\times 10^{-4}$ rad/mm)	$\mu_{\Delta u} = \frac{\Delta_2}{\Delta_{yI}}$	$\mu_{\varphi u} = \frac{\Phi_2}{\Phi_{yI}}$	E_N
1	C-A	40	C	1.42	779	8.52	2.25	3.69	15.0	9.5
	L-C-S	40	C	1.00	549	8.23	2.94	3.64	14.7	10.0
2	D-A	46	D	1.42	779	13.62	3.56	4.38	17.8	9.6
	L-D-S	46	D	1.00	549	8.73	3.15	3.70	15.0	11.4

specimens L-C-S and C-S, in which transverse reinforcement spacing was 40 and 57 mm, respectively. Both specimens had 100 % of required areas of transverse reinforcement, as specified by the seismic provisions of ACI 318-02. However, the first specimen showed higher ductility. The use of higher grade steel for transverse reinforcement could satisfy ACI 318-02 requirements while having larger spacing of ties. However, at the same time, larger spacing could result in a lower ductile behaviour, as shown in Fig. 7.

(4) Flexural strength

There is not universal agreement on the applicability of ACI 318-02 code requirements for calculating the flexural strength of HSC column sections subject to combined axial load and bending moment.

Columns are usually designed for combined axial load and bending moment using the rectangular stress block defined in ACI 318-02 Section 10.2.7. This stress block was originally derived by Mattock et al.[12], based on tests

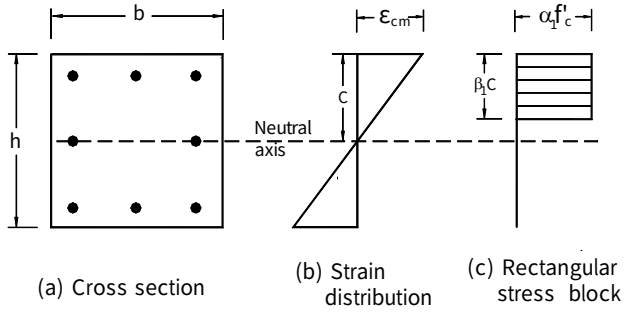

Figure 12. Concrete equivalent stress block

of un-reinforced concrete columns loaded with axial load and moments. The concrete strengths ranged up to 52.5 MPa. The stress block was defined by two parameters: the intensity of stress in the stress block, which was designated as α_1; and the ratio of the depth of the stress block to the neutral axis, which was designated as β_1 (Fig. 12).

Mattock et al.[12] proposed $\alpha_1 = 0.85$, and β_1 as follows:

$$\beta_1 = 1.05 - 0.05(f_c'/6.9) \le 0.85 \quad (6)$$

for f_c' in MPa. That proposal was incorporated into Section 1504g of ACI 318-63. Based on similar tests of concrete columns with concrete strength ranging from 79 to 98 MPa, Nedderman [13] proposed a lower limit on β_1 of 0.65 for concrete strength in excess of 55 MPa. This limit was incorporated in ACI 318-77.

Bing et al.[14] have suggested that an equivalent rectangular compressive stress block with an average stress, $\alpha_1 f_c$', and a depth, $a = \beta_1 c$, be used in the design of HSC column cross-sections, where:

$$\alpha_1 = 0.85, \text{ for } f_c' \le 55 \text{ MPa} \quad (7)$$

and

$$\alpha_1 = 0.85 - 0.004(f_c'-55) \ge 0.75, \text{ for } f_c' > 55 \text{ MPa} \quad (8)$$

Azizinamini et al.[15] recommend that the following equivalent rectangular compression block be adopted for calculating the nominal moment strength of concrete columns with f_c' exceeding 70 MPa and designed according to seismic provisions of ACI 318-02. When f_c' exceeds 70 MPa, the stress intensity of an equivalent rectangular compression block must be decreased linearly from 0.85 to 0.6, using the expression

$$\alpha_1 = 0.85 - 0.0073(f_c'-69) \ge 0.6 \quad (f_c' \text{ in MPa}) \quad (9)$$

Table 7. Comparison of calculated and experimental flexural strengths

Specimen	S (mm)	Detail	ρ_s (%)	$\frac{\rho_S}{\rho_{(ACI)}}$	f_{yh} (MPa)	M_{EXP} (kN.m)	$\frac{M_{EXP}}{M_{ACI}}$	$\frac{M_{EXP}}{M_{Ibrahim}}$	$\frac{M_{EXP}}{M_{Bing}}$	$\frac{M_{EXP}}{M_{Azizina\min i}}$
C-S	57	C	1.58	1.00	779	98.0	1.15	1.18	1.23	1.25
D-S	65	D	1.58	1.00	779	95.2	1.12	1.17	1.19	1.22
H-S	38	H	1.58	1.00	779	97.3	1.14	1.17	1.22	1.24
C-A	40	C	2.25	1.42	779	105.2	1.24	1.27	1.32	1.34
D-A	46	D	2.25	1.42	779	98.0	1.15	1.18	1.23	1.25
H-A	27	H	2.25	1.42	779	96.6	1.14	1.16	1.21	1.24
L-C-S	40	C	2.25	1.00	549	94.4	1.11	1.14	1.18	1.21
L-D-S	46	D	2.25	1.00	549	93.9	1.10	1.13	1.17	1.20

Ibrahim et al.[16] compared the concrete component of the measured load and moment strengths of 94 tests of eccentrically loaded columns and proposed the following equation:

$$\alpha_1 = (0.85 - 0.00125\, f_c') \geq 0.725 \quad (f_c' \text{ in MPa}) \qquad (10)$$

and

$$\beta_1 = (0.95 - 0.0025\, f_c') \geq 0.70 \quad (f_c' \text{ in MPa}) \qquad (11)$$

Table 7 gives a summary of maximum measured and calculated moments for test columns. In general, the ACI 318-99 provisions gave a conservative prediction of the nominal moment capacity of test columns with f_{ck} at 69 MPa. The ratios of measured to nominal moment capacities as predicted by ACI 318-02 provisions ranged from 1.10 to 1.24 for columns with f_{ck} at 69 MPa. Table 7 also gives nominal moment capacity calculated using the stress blocks suggested by Bing, Azizinamini and Ibrahim [14-16]. As shown in Table 7, these approaches also result in conservative predictions of test column flexural capacity, as the ratios of measured over predicted values vary from 1.13 to 1.34.

For members subjected to pure flexural loads, it has been reported [17] that the current ACI 318-02 provision could be extended to predict moment capacities of HSC members. This could very well be true since, when a cross-section is subjected to a bending moment only, the depth of the neutral axis at ultimate conditions is generally small and the shape of the compressive block becomes less important. However, in the case of columns, the depth of the neutral axis is a significant portion of the member's overall depth, making the nominal moment capacity more sensitive to the assumed shape of the compression block.

5. CONCLUSIONS

Based on the experimental investigations reported, the following conclusions were reached.

1. The hysteretic behavior of the HSC columns can be characterized by three distinct stages: 1) the initial stage with the full participation of both confined core concrete and unconfined cover concrete; 2) stable behavior with deformation contributed primarily by longitudinal steel yielding and straining of confined core concrete; and 3) final failure.

2. Specimens made of high-strength concrete with f_{ck} around 69 MPa, confined with more than 42% of the transverse reinforcement required by the ACI 318-02, can be made to behave in a ductile manner, showing a displacement ductility factor ($\mu_{\Delta u}$) of 4 and a curvature ductility factor ($\mu_{\varphi u}$) of over 15.

3. In general, the ACI 318-02 provisions give a conservative prediction of the nominal moment capacity of test columns with f_{ck} at 69 MPa as the ratios of measured over predicted values range from 1.10 to 1.24. Nominal moment capacity calculated using the stress blocks suggested by Ibrahim, Bing and Azizinamini also conservatively predict the nominal moment capacity of the test columns.

4. The use of high-strength material for transverse reinforcement (779 MPa) in HSC columns was not beneficial when axial load ratio (P/P_O) was 0.3. Therefore, for axial-load levels below 30% of the column's axial capacity, it is suggested that the yield strength of transverse reinforcement be held equal to or below 549 MPa.

5. For specimens with the same volumetric ratio of transverse reinforcement, specimens with type-H ties display more ductile behaviour than specimens with type-C or type-D ties.

REFERENCES

Russell, H. B., "High Strength Concrete in North America," Proceedings of Symposium on Utilization of High Strength Concrete, Stavanger, Norway, June 15-18, 1987.

Shah, S. P.; Zia, P.; and Johnson, D., "Economic Considerations for Using High Strength Concrete in High Rise Buildings," study prepared for Elborg Technology Co., Dec. 1983

Smith, J., and Rad, F. N., "Economic Advantages of High-Strength Concrete in Columns, Concrete International:

Design & Construction, V.11, No. 4, 1989, pp. 25-92.
"Uniform Building Code," International Conference of Building Officials, Whittier, 1988.
Sakai, K., and Sheikh, S.A., "What Do We Know about Confinement in Reinforced Concrete Columns?," ACI Structural journal, V.86, No.2, Mar.-Apr. 1989, pp. 192-201.
Martinez, S.; Nilson, A. H.; and Slate, F. O., "Spirally Reinforced High-Strength Concrete Columns," ACI Structural journal, V.81, No.5, Sept.-Oct. 1984, pp. 431-442.
Basset, R., and Uzumeri, S. M., "Effect of Confinement on the Behaviour of High-Strength Lightweight Concret Columns," Canadian Journal of Civil Engineers, V.13, 1986
ACI-ASCE Committee 441, "High-Strength Concrete Columns : State of the Art," ACI Structural Journal, V.94, No. 3, May-June 1997. pp. 325-335.
Newmark, N. M., and Hall W. J., Earthquake Spectra and Design, Earthquake Engineering Research Institute, Berkeley, Calif., 1980, 103 pp.
Sheikh, S. A., and Khoury, S.S., "Confined Concrete Columns with Stubs, "ACI Structural Journal, V. 90, No. 4, Sept.-Oct. 1993, pp. 414-431.
Park, R., "Evaluation of Ductility of Structures and Structural Assemblages from Laboratory Testing, "Bulletin of the New Zealand National Society for Earthquake Engineering, V.22, No.3, 1989, pp. 155-166.
Mattock, A.H., Kriz, L.B.,and Hognestad, E., "Rectangular Concrete Stress Distribution in Ultimate Strength Design", ACI Journal, Proceeding, V.57, No.8, Feb. 1961, pp.875-928.
Nedderman,H., "Flexural Stress Distribution in Very High Strength Concrete", MSc Thesis, University of Texas Arlington, December 1973, 182pp
Bing, Li, Park,R, and Tanka , H., "Effect of Confinement on the Behaviour of High-Strength Concrete Columns under Seismic Loading", Pacific Conference on Earthquake Engineering, New Zealand, Nov.1991
Azizinamini, A., Kuska,S, Brungardt, P., and Hatfeild, E., "Seismic Behaviour of Square High-Strength Concrete Columns", ACI Journal, V.91, No.3,May-Jun. 1994, pp.336-345.
Ibrahim, Hisham, and MacGregor, James G., " Flexural Behaviour of High-Strength Concrete Columns", Structural Engineering Report No.196 University of Alberta, Edmonton, Alberta, March, 1994
Shin, S. W. ; Ghosh, S. K. ; and Moren, J., "Flexural Ductility of Ultra-High-Strength Concrete Members, "ACI Structural Journal, V. 86, No. 4, July-Aug, 1989. pp. 394-400.
Lee, J. H.; Ko, S. H.; Lee, D. H.; Chung, Y. S., "Flexure-Shear Behavior of Circular Columns under Cyclic Lateral Loads", Journal of the Korea Concrete Institute , V. 16, No. 6, Dec, 2004, pp. 823-832.
Lee, J. H.; Kim, K. S.; Bae, S. Y.; Yun, S. K., "Characteristic of High-Strength Concrete Spiral Bridge Columns under Simulated Seismic Loading", Journal of the Korean Society Concrete Engineering , V. 21, No. 5-A, Sep, 2001, pp. 707-718.
Shin, S. W.; Ahn, J. M.; Han, B. S.; Lee, K. S.; "The Behavior of High-Strength R/C Columns Subjected to Reversed Cyclic and Axial Force", Journal of the Architectural Institute of Korea, V. 15, No. 2, Feb, 1999, pp. 47-54.

NOTATION

ρ_s = volumetric ratio of lateral reinforcement
ρ_t = volumetric ratio of longitudinal reinforcement
f_y = yielding stress of longitudinal reinforcement
f_{yh} = yielding stress of lateral reinforcement
f_u = ultimate stress of reinforcing steel
f_c ' = cylinder compressive strength of concrete specimen
E_s = modulus of elasticity of reinforcing steel
α_1= coefficient that defines width of rectangular stress block
β_1= coefficient that defines height of rectangular stress block
P= axial load carried by concrete
P_o = nominal axial-load capacity of column: $P_o = 0.85(A_g - A_{st})f_c' + A_s f_y$
Δ = tip displacement of column
Δ_2 = maximum displacement of column
Δ_{1y} = ideal yield displacement of column
Φ = curvature
Φ_2 = maximum curvature
Φ_{1y} = ideal yield curvature
$\mu_{\Delta u}$ = ultimate displacement ductility
$\mu_{\Phi u}$ = ultimate curvature ductility

(Data of Submission : 2005. 1.14)